Solvation energies and electronic spectra in polar, polarizable media: Simulation tests of dielectric continuum theory

Joel S. Bader and B. J. Berne

Citation: The Journal of Chemical Physics **104**, 1293 (1996); doi: 10.1063/1.470787
View online: http://dx.doi.org/10.1063/1.470787
View Table of Contents: http://scitation.aip.org/content/aip/journal/jcp/104/4?ver=pdfcov
Published by the AIP Publishing

Solvation energies and electronic spectra in polar, polarizable media: Simulation tests of dielectric continuum theory

Joel S. Bader[a)]
Department of Chemistry, Columbia University, New York, New York 10027

B. J. Berne[b)]
Institute of Physics, University of Augsburg, Memminger Str. 6, D-86135 Augsburg, Germany

(Received 28 July 1995; accepted 17 October 1995)

A dielectric continuum theory for the solvation of a polar molecule in a polar, polarizable solvent is tested using computer simulations of formaldehyde in water. Many classes of experiments, for example those which measure solvent-shifted vertical transition energies or electron transfer rates, require an explicit consideration of the solvent electronic polarization. Due to the computational cost of simulating a polarizable solvent, many simulation models employ non-polarizable solute and solvent molecules and use dielectric continuum theory to relate the properties of the non-polarizable system to the properties of a more realistic polarizable system. We have performed simulations of ground and excited state formaldehyde in both polarizable and non-polarizable water, and the solvation energies and solvent-shifted electronic spectra we obtained are used to test dielectric continuum, linear response predictions. Dielectric continuum theory correctly predicts that free energy differences are the same in polarizable and non-polarizable water. The theory wrongly predicts that the reorganization energy in a polarizable solvent is 30% smaller than the reorganization energy in a polar, non-polarizable solvent; in the simulations, the reorganization energies differ by only 6%. We suggest that the dielectric continuum theory fails because it assumes that both solute electronic states exist in the same size cavity in the solvent, whereas in the simulation the cavity radius increases by 20% after the electronic transition. We account for the change in the cavity size by adding a non-linear solute–solvent coupling to the dielectric continuum theory, and find that the resulting predictions are just outside the error bounds from the simulation. The cavity size corrections have the undesired and incorrect side-effect of predicting fluctuations far smaller than seen in the simulations. This reveals the inherent difficulty in devising a simple, fully self-consistent dielectric continuum theory for solvation. © *1996 American Institute of Physics.* [S0021-9606(96)50604-4]

I. INTRODUCTION

In solution state electronic spectroscopy, a solute molecule immersed in solvent is excited by a photon from its ground electronic state to an excited electronic state. An example of this is the $n \rightarrow \pi^*$ transition of formaldehyde in water. The ground and excited states of the formaldehyde molecule have different electronic structure and thus have different interactions with the solvent. The vertical transition energy reflects the difference in the energy of interaction between the ground and excited state electronic distributions with the instantaneous configuration of the solvent molecules. The absorption line shape will then be given by the distribution function of the vertical transition energies found when the solvent molecules can sample all of the configurations in equilibrium with the ground electronic state of formaldehyde. The fluorescence spectrum can likewise be related to the distribution of vertical transition energies when the solvent configurations are sampled from a distribution in equilibrium with the excited state.

In modeling the photophysics of solvated molecules it is common to treat the solvent as non-polarizable. Of course real solvents are polarizable, and the issue we address here is the importance of considering the electronic polarizability explicitly. For example, a comparison of gas phase properties to liquid phase properties demonstrates the importance of including induced electric polarization. Water, for instance, has a gas phase dipole moment of 1.85 D.[1] In liquid water, however, the dipole moment is enhanced. The exact magnitude of the dipole is unknown, but is thought to be close to 2.4 D based on the known dipole moment of 2.6 D for molecules in ice.[2] Thus, there are two contributions to the instantaneous dipole moment of a molecule in the liquid state: first, a permanent dipole characteristic of the gas phase; second, a fluctuating induced dipole due to collective effects from the surrounding molecules.

One aim of this paper is to understand the contribution to the solvent shift that is made by solvent polarizability arising from the fluctuating, induced dipoles of solvent molecules. The induced polarization responds instantly during an electronic transition, and the solvent shift should be different from the shift obtained in a non-polarizable solvent. In Sec. II, we present a simple theory for relating solvent shifts in polar, polarizable and polar, non-polarizable solvents. This

[a)]Permanent address: CuraGen Corporation, 322 East Main Street, Branford, Connecticut 06405.
[b)]Permanent address: Department of Chemistry, Columbia University, New York, New York 10027.

theory is based on the Marcus picture of electron transfer reactions, in which solute electronic states are coupled linearly to a harmonic solvent,[3–6] and is in fact a spin-Boson model.[7] The theory is patterned after recent advances which explicate the role of solvent electronic polarization in charge transfer reactions.[8–14] The theoretical model we employ permits us to predict the contributions of orientational polarization and of induced electronic polarization to the solvent shifts for absorption or fluorescence lines, to equilibrium free energies of solvation, and to non-equilibrium solvent reorganization energies. Furthermore, the linear nature of the theory implies that it is equivalent at a fundamental level to a dielectric continuum treatment of the solvent, which also assumes linear response.[15–20] Dielectric continuum theory is also the basis of the Poisson and Poisson–Boltzmann equations for the response of a continuum solvent to a solute. Various methods for obtaining numerical solutions to these equations have found widespread use as substitutes for molecular solvents in computational studies.[21–25] Although other studies have focused on the quantitative accuracy of these methods per se,[26–30] our interest here is in the fundamental adequacy of this approach when it is used to treat the electronic polarization of the solvent.

Simulation studies using polarizable solvent molecules have offered valuable insight to the contribution of the electronic polarization modes to the solute–solvent interactions.[31–38] Here we use simulations to test the predictions of a linear response, dielectric continuum model for the formaldehyde-water system. We used four different models of water in the simulations: the TIP4P-FQ (fluctuating charge),[39] MQ (mean charge), FQ/MQ (a hybrid in which solvent conformations are taken from FQ simulations but solute-solvent interactions are evaluated using the fixed MQ charges), and TIP4P (Ref. 40) models. The FQ model is polarizable; the MQ and TIP4P models are not polarizable. As will be described in Sec. III A, the MQ model is derived from the FQ model by replacing the fluctuating charges with fixed charges characteristic of bulk TIP4P-FQ water. Our model for formaldehyde, based on the work of Levy and coworkers,[41–43] is non-polarizable. The formaldehyde model is discussed in Sec. III B.

Our simulation results for absorption and fluorescence line shapes are presented and discussed in Sec. IV, and compared to dielectric continuum theory predictions. The parameters used in the dielectric continuum theory are the high-frequency and low-frequency limits of the solvent dielectric constant, the dipole moment of the solute in each electronic state, and the effective radius of the solute molecule. The free energy changes predicted by dielectric continuum theory agree with the simulation results, but the predicted reorganization energies are 30% smaller than the simulation results.

One important source of the disagreement between theory and simulation is the theoretical assumption that the effective radius of the solute is identical in the ground state and the excited state. In the simulations, however, this radius is seen to increase by about 20% following equilibration of the water to the excited state formaldehyde molecule. It is possible to allow the effective radius to depend on the solute electronic state by introducing a non-linear solute–solvent coupling to the dielectric continuum theory. This theory is described in Sec. II E. The predictions of the non-linear theory for the reorganization energy are greatly improved and lie just outside the statistical error bars of the simulation results. The non-linear theory is also applied to calculate spectral linewidths, which characterize the solvent fluctuations. Unlike the linewidths from the fully linear theory, which are in good agreement with simulation results, the linewidths from the non-linear theory are far narrower than the simulation results. This seems to point out a basic inconsistency in the dielectric continuum theory.

II. THEORY

A. The ubiquitous spin-boson Hamiltonian

A simplified description of the solute–solvent system begins with a model for the pure solvent. Here we assume that the solvent can be represented as a dielectric continuum. A standard assumption in most applications of dielectric continuum theory is that the dielectric responds linearly to an applied field. Linear response implies that the effective Hamiltonian for a dielectric continuum solvent can be represented as a collection of harmonic oscillators chosen at a spectrum of frequencies to reproduce the frequency-dependent dielectric constant. Instead of a full frequency spectrum, we will partition the solvent response into two frequency regimes: low frequency (classical) and high frequency (quantum mechanical). The Hamiltonian for the pure bath is therefore

$$H_B=\frac{1}{2\alpha_0}\mathscr{E}_0^2+\frac{1}{2}\alpha_0\omega_0^2\Pi_0^2+\frac{1}{2\alpha_\infty}\mathscr{E}_\infty^2 + \frac{1}{2}\alpha_\infty\omega_\infty^2\Pi_\infty^2-\frac{1}{2}\hbar\omega_\infty . \tag{1}$$

The coordinate of the slow mode is $\mathscr{E}_0$, its polarizability is α_0, the momentum conjugate to $\mathscr{E}_0$ is Π_0, and the frequency of the mode is ω_0. Since $\mathscr{E}_0$ represents classical modes, the frequency ω_0 is much smaller than the thermal energy k_BT. The induced polarization is represented by the effective coordinate $\mathscr{E}_\infty$. This mode is high frequency, $\omega_\infty \gg k_BT$. The polarizability of $\mathscr{E}_\infty$ is α_∞, and the conjugate momentum is Π_∞. The zero-point energy of the mode $\mathscr{E}_\infty$ has been taken as the zero of energy. In terms of a molecular solvent, $\mathscr{E}_0$ corresponds to the polarization of slow, orientational modes, and $\mathscr{E}_\infty$ corresponds to fluctuations of the induced polarization of the electron charge density of solvent molecules.

The ground and excited electronic states of the solute are represented by a two level system (TLS) which couples linearly to the bath:

$$H=H_B+H_{\mathrm{TLS}}+V; \tag{2a}$$

$$H_{\mathrm{TLS}}=|1\rangle E_1\langle 1|+|2\rangle E_2\langle 2|-K(|1\rangle\langle 2|+|2\rangle\langle 1|); \tag{2b}$$

$$V=-(\mathscr{E}_0+\mathscr{E}_\infty)\cdot(|1\rangle Q_1\langle 1|+|2\rangle Q_2\langle 2|). \tag{2c}$$

The energies E_1 and E_2 are the gas-phase, unsolvated energies of the solute ground and excited states. The two states are coupled by the term in H_{TLS} proportional to K, allowing non-adiabatic transitions to occur. The terms Q_1 and Q_2 represent the solute coordinate which couples to the solvent. For the case of formaldehyde, Q_1 and Q_2 represent the ground and excited state dipoles of the formaldehyde molecule.

The generic form of the Hamiltonian in Eq. 2 is that of a two level system coupled to a bath of harmonic oscillators. This is, of course, the well-known spin-Boson Hamiltonian which serves as the basis for most theories in which two different electronic states are allowed to interact with a solvent. Here our solvent has only two modes, a slow classical mode representing orientational polarization of solvent molecules, and a fast quantum mechanical mode representing the electronic polarization of the solvent molecules. The spin-Boson model has had wide use as a model for charge transfer reactions, particularly in understanding effects due to the quantum nature of solvent modes.[10–14,44–50]

Because the frequency ω_∞ is very large, a Born–Oppenheimer separation is valid for the mode $\mathscr{E}_\infty$. We assume that this mode remains in its ground state. The adiabatic separation of the fast mode $\mathscr{E}_\infty$ yields a pair of adiabatic states with renormalized energies:

$$H=|1\rangle H_1\langle 1|+|2\rangle H_2\langle 2|-K(|1\rangle\langle 2|+|2\rangle\langle 1|); \tag{3a}$$

$$H_1=E_1-\frac{1}{2}\alpha_\infty Q_1^2+\frac{1}{2\alpha_0}\mathscr{E}_0^2-\mathscr{E}_0\cdot Q_1+\frac{1}{2}\alpha_0\omega_0^2\Pi_0^2; \tag{3b}$$

$$H_2=E_2-\frac{1}{2}\alpha_\infty Q_2^2+\frac{1}{2\alpha_0}\mathscr{E}_0^2-\mathscr{E}_0\cdot Q_2+\frac{1}{2}\alpha_0\omega_0^2\Pi_0^2. \tag{3c}$$

The two diabatic states are coupled by the term proportional to K.

The bath Hamiltonian H_B we used in obtaining the Born–Oppenheimer states is very similar to model Hamiltonians which have been used previously in a similar context.[10,11] In some formulations, H_B contains a term $-k\mathscr{E}_0\cdot\mathscr{E}_\infty$ linearly coupling the fast and slow modes. In Appendix A we show that the two formulations are equivalent for our purposes. Including a term which linearly couples $\mathscr{E}_0$ and $\mathscr{E}_\infty$ serves to shift the equilibrium position of $\mathscr{E}_\infty$, to rescale the polarizability α_0, and to rescale the terms $-\mathscr{E}_0\cdot Q_1$ and $-\mathscr{E}_0\cdot Q_2$. In taking $\mathscr{E}_0$ and $\mathscr{E}_\infty$ to be uncoupled normal modes of the solvent, we have included this renormalization as a first step.

The potential energy curves for the two diabats, V_1 and V_2, are shown in Fig. 1 as functions of the solvent coordinate $\mathscr{E}_0$. These are the standard intersecting parabolas of Marcus theory. The difference in free energy between the two states, ΔG_{21}, is marked on the curve, as is the solvent reorganization energy λ. As will be shown below, the free energy difference includes contributions from polarizable and non-polarizable modes, but the reorganization energy λ only contains contributions from non-polarizable modes. The center of the absorption band, ΔE_{21}, is shown, as is the center of the fluorescence band, ΔE_{12}. These quantities will be related to parameters appearing in the spin-Boson Hamiltonian. But first, we will make a few phenomenological connections between the Hamiltonian parameters representing the polarizability and the physical quantity which characterizes equilibrium solvation, i.e. the individual solvation energies ΔG_1 and ΔG_2.

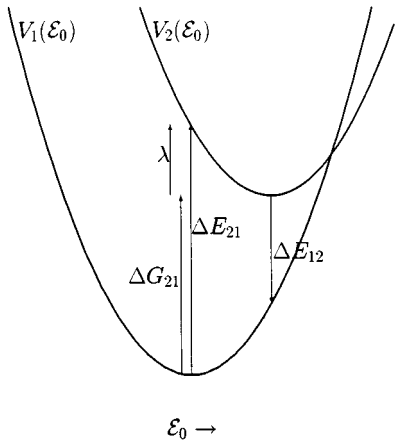

FIG. 1. The potential energy surfaces V_1 and V_2 for two diabatic electronic states are shown as a function of the solvent coordinate $\mathscr{E}_0$. The free energy difference between the states, which includes contributions from polarizable solvent modes, is ΔG_{21}. The solvent reorganization energy, which only includes contributions from the classical mode $\mathscr{E}_0$, is λ. The center of the absorption band is ΔE_{21} and the center of the fluorescence band is ΔE_{12}.

B. Solvation free energies

The solvation energy ΔG_i for electronic state $i=1$ or 2 corresponding to the transition $CH_2O^{(g)}\rightarrow CH_2O^{(aq)}$ is defined as

$$\Delta G_i=-k_BT\ \ln\{\mathrm{Tr}e^{-\beta H_i}/\mathrm{Tr}e^{-\beta(H_B+E_i)}\}. \tag{4}$$

The trace is over the modes of the bath, and the solute is held fixed in electronic state i. The fast modes of the bath are included in the trace over H_B, but have already been integrated over in the diabatic Hamiltonian H_i. As before, the gas-phase energy of the solute in state i is E_i. It is a simple matter to use Eqs. 1 and 2 to evaluate ΔG_i, yielding the result

$$\Delta G_i=-\frac{1}{2}(\alpha_\infty+\alpha_0)Q_i^2. \tag{5}$$

Using this expression for ΔG_i, we can relate the polarizabilities α_0 and α_∞ to well-defined physical properties of the solvent.

The solvent properties which we consider are the (low frequency) static dielectric constant, ϵ_0, and the (high frequency) optical dielectric constant, ϵ_∞. The precise relationship between the polarizability and the dielectric constant also depends on the type of electrostatic moment that is represented by the solute parameters Q_1 and Q_2, and on the shape of the cavity representing the solute. Suppose, for ex-

ample, that the solute is a spherical molecular monopole of radius R immersed in a dielectric continuum, and that Q_i represents a charge on the molecule. In this case, the solvation energy is given by the Born equation[15,20]

$$\Delta G_i = -\frac{1}{2} R^{-1}[(\epsilon_0 - 1)/\epsilon_0] Q_i^2 \tag{6}$$

indicating from Eq. 5 that

$$\alpha_0 + \alpha_\infty = R^{-1}[(\epsilon_0 - 1)/\epsilon_0]. \tag{7a}$$

This response represents the equilibrium solvation of a charge distribution. In order to calculate absorption and fluorescence line shapes, we also need to understand the instantaneous response of the solvent which arises from the modes contributing to α_∞.

We can separate the contributions of the fast modes from those of the slow modes by imagining a solute which oscillates rapidly between the charges $+Q_i$ and $-Q_i$. In this case, the mode $\mathscr{E}_0$ cannot respond to the solute charge and makes no contribution to the solvation energy. The fast mode $\mathscr{E}_\infty$ is assumed to provide full solvation at each instant, from which it follows that

$$\alpha_\infty = R^{-1}[(\epsilon_\infty - 1)/\epsilon_\infty], \tag{7b}$$

and

$$\alpha_0 = R^{-1}[(\epsilon_0 - 1)/\epsilon_0 - (\epsilon_\infty - 1)/\epsilon_\infty]. \tag{7c}$$

The low frequency polarizability has been obtained by subtraction.

Similar equations are obtained when each Q_i represents a point dipole in a spherical cavity of radius R:[20]

$$\alpha_0 + \alpha_\infty = R^{-3}[2(\epsilon_0 - 1)/(2\epsilon_0 + 1)]; \tag{8a}$$

$$\alpha_\infty = R^{-3}[2(\epsilon_\infty - 1)/(2\epsilon_\infty + 1)]; \tag{8b}$$

$$\alpha_0 = R^{-3}[2(\epsilon_0 - 1)/(2\epsilon_0 + 1) - 2(\epsilon_\infty - 1)/(2\epsilon_\infty + 1)]. \tag{8c}$$

It is possible to continue the analysis of α_0 and α_∞ for the response to higher moments in the multipole expansion, and to more complicated solute geometries. This is typically accomplished by solving the Poisson or Poisson–Boltzmann equation for the response of a continuum solvent to the charge distribution and geometry of an immersed solute.[51] We have applied these methods to our model of formaldehyde in water.[52] We do not report the quantitative results of continuum theory here because our present interest is to understand the qualitative difference between solvation with and without electronic polarizability.

The above equations can be summarized by introducing a function $f(\epsilon)$ defined as

$$f_n(\epsilon) = \begin{cases} (\epsilon - 1)/\epsilon, & \text{monopole solvation } (n=1); \\ 2(\epsilon - 1)/(2\epsilon + 1), & \text{dipole solvation } (n=2). \end{cases} \tag{9}$$

With this definition, the polarizabilities are given by

$$\alpha_{\text{tot}} \equiv \alpha_0 + \alpha_\infty = R^{-(2n-1)} f_n(\epsilon_0); \tag{10a}$$

$$\alpha_\infty = R^{-(2n-1)} f_n(\epsilon_\infty); \tag{10b}$$

and

$$\alpha_0 = R^{-(2n-1)}[f_n(\epsilon_0) - f_n(\epsilon_\infty)]. \tag{10c}$$

The cavity radius is R and the index n is 1 for monopole solvation and 2 for dipole solvation.

C. Line shapes and energies with the linear coupling Hamiltonian

The mean energy for a vertical transition from state 1 to state 2 is termed ΔE_{21},

$$\Delta E_{21} = \langle H_2 - H_1 \rangle_1 \tag{11a}$$

$$= -\frac{1}{2}\alpha_\infty (Q_2^2 - Q_1^2) - \alpha_0 Q_1 \cdot (Q_2 - Q_1) + E_2 - E_1. \tag{11b}$$

The subscript "1" on the average indicates that the average is taken in diabatic state 1, and we have used the fact that $\langle \mathscr{E}_0 \rangle_1 = \alpha_0 Q_1$. We have also assumed that the coupling K is small compared to ΔE_{21} and can be ignored. The gas-phase transition is at constant energy $E_2 - E_1$, and the remainder of ΔE_{21} represents the solvent shift in the observed transition.

Since the mode $\mathscr{E}_0$ is harmonic, the shift due to the solvent is governed by a Gaussian distribution. The absorption line shape is also a Gaussian,

$$P_{2\leftarrow 1}(E) = (2\pi\sigma_0^2)^{-1/2} \exp[-(E - \Delta E_{21})^2/2\sigma_0^2]. \tag{12}$$

The width of the line is σ_0,

$$\sigma_0 = \sqrt{k_B T \alpha_0}\,|Q_2 - Q_1|. \tag{13}$$

An analogous result is obtained for the mean energy ΔE_{12} for the fluorescence back to state 1, assuming that equilibration has occurred on surface 2:

$$\Delta E_{12} = \langle H_1 - H_2 \rangle_2 \tag{14a}$$

$$= -\frac{1}{2}\alpha_\infty (Q_1^2 - Q_2^2) - \alpha_0 Q_2 \cdot (Q_1 - Q_2) + E_1 - E_2. \tag{14b}$$

Correspondingly, the fluorescence line shape is

$$P_{1\leftarrow 2}(E) = (2\pi\sigma_0^2)^{-1/2} \exp[-(E - \Delta E_{12})^2/2\sigma_0^2]. \tag{15}$$

From Eqs. 12, 13, and 15 we see that the solvent shifts in the absorption and emission lines depend on both α_∞ and α_0, but the widths of the spectral lines depend only on α_0. Furthermore, the widths of the absorption and fluorescence are the same. This behavior is depicted in schematic form in Fig. 2. The absorption spectrum for a solute molecule in the gas phase is represented as a δ-function in the figure. Next, we imagine that the solute is immersed in a solvent with total polarizability α_{tot}. Furthermore, the entire solvent response is assumed to arise from electronic polarizability, so $\alpha_\infty/\alpha_{\text{tot}} = 1$. In this solvent, the absorption line shape remains a δ-function, but it is shifted from the gas phase line. The direction of the shift is towards higher energy if the excited state is less polar than the ground state, and it is towards lower energy if the excited state is more polar than the ground state. Keeping the total polarizability α_{tot}

constant, we reduce the contribution of α_∞ and increase the contribution of slow modes α_0 to the solvent response. As the contribution of the slow modes increases, the center of the absorption line continues to shift with a corresponding broadening of the line shape from a δ-function to a Gaussian. As is seen clearly in the figure, the width of the Gaussian increases as the contribution of the slow modes increases. This is because the width is proportional to $\sqrt{\alpha_0}$.

The vertical transition energies ΔE_{21} and ΔE_{12} measure the sum of a gas-phase energy difference and a non-equilibrium solvation energy difference. In ΔE_{21}, for example, the energy of state 2 is measured with the slow coordinate $\mathscr{E}_0$ in equilibrium with state 1. It is also possible to measure a free energy difference at full equilibrium in both states. This free energy difference is denoted ΔG_{21},

$$\Delta G_{21} = -k_B T \ln\{\mathrm{Tr}_{\mathscr{E}_0} \exp[-\beta H_2]/\mathrm{Tr}_{\mathscr{E}_0} \exp[-\beta H_1]\}$$
$$= \Delta G_2 - \Delta G_1 + (E_2 - E_1). \tag{16}$$

One finds that

$$\Delta G_{21} = -\frac{1}{2}(\alpha_\infty + \alpha_0)(Q_2^2 - Q_1^2) + E_2 - E_1 \tag{17a}$$

$$= \frac{1}{2}(\Delta E_{21} - \Delta E_{12}). \tag{17b}$$

The equilibrium response is determined by $\alpha_{\mathrm{tot}} \equiv \alpha_0 + \alpha_\infty$, the sum of the response of the fast and the slow modes.

The difference between ΔE_{21}, the non-equilibrium difference in energy, and ΔG_{21}, the fully equilibrated free energy difference, is termed the reorganization energy λ:

$$\lambda = \Delta E_{21} - \Delta G_{21} \tag{18a}$$

$$= \frac{1}{2}(\Delta E_{21} + \Delta E_{12}) \tag{18b}$$

$$= \frac{1}{2}\alpha_0 (Q_2 - Q_1)^2. \tag{18c}$$

From Eq. 13, the spectral line width σ_0 is related to the reorganization energy by

$$\sigma_0^2 = 2\lambda k_B T. \tag{19}$$

It is seen explicitly in Eq. 18c that the reorganization energy depends only on the slow modes. The fast modes contribute to ΔE_{21} and to ΔG_{21}, but the contributions are identical and cancel when λ is calculated as their difference. The gas-phase contribution to ΔE_{21} and ΔG_{21} also cancels when λ is calculated. The reorganization energy is seen to be a positive quantity and is the same for both the $2 \leftarrow 1$ transition and the $1 \leftarrow 2$ transition.

This definition of λ is entirely consistent with the conventions of electron transfer theory. The activation energy for a thermal transition from state 1 to state 2, for example, is

$$E_{\mathrm{act}} = (\Delta G_{21} + \lambda)^2 / 4\lambda, \tag{20}$$

assuming that the coupling K is small and the reaction is in the non-adiabatic regime.[5]

D. The difference between polarizable and non-polarizable solvents

We will assume the existence of two hypothetical solvents which share the same equilibrium response, i.e. the same ϵ_0 and α_{tot}, but different values for α_0 and α_∞. In particular, we will compare a polarizable solvent with non-zero α_∞ to a non-polarizable solvent with $\alpha_\infty \to 0$. These hypothetical solvents can be modeled by computer simulations. The polarizable TIP4P-FQ model of water and various non-polarizable water models, including the models which we consider here (MQ, FQ/MQ, and TIP4P), typify a collection of solvents with a similar equilibrium response but with different high-frequency response. All four of these solvents have a static dielectric constant close to the experimental value $\epsilon_0 = 80$. Since α_{tot} depends only on ϵ_0, these models share the same α_{tot}. Because ΔG_{21} depends only on α_{tot}, these models should both produce the same estimates for differences in solvation free energy.

The four models have very different high frequency responses, however. The TIP4P-FQ model has an optical dielectric constant of 1.59, indicating that it has an instantaneous polarization response. The fixed-charge models, MQ, FQ/MQ, and TIP4P, are all non-polarizable. For these three models, $\alpha_\infty = 0$, and ϵ_∞ has the trivial value of 1. Because the short-time response of the polarizable water model is different from the short-time response of the non-polarizable models, we would expect that an experiment which probes short-time dynamics (such as the instantaneous solvent response during an electronic transition of a solute molecule) should reveal differences between the behavior of polarizable versus non-polarizable solvent models.

Furthermore, when the reorganization energy λ is considered, a clear difference arises between the polarizable and non-polarizable solvents in the dielectric continuum theory. The total polarizability of the two solvents is assumed to be the same, $\alpha_{\mathrm{tot}}^{(\mathrm{pol})} = \alpha_{\mathrm{tot}}^{(\text{non-pol})}$. For the non-polarizable solvent, $\alpha_\infty^{(\text{non-pol})} = 0$ and hence $\alpha_0^{(\text{non-pol})} = \alpha_{\mathrm{tot}}^{(\text{non-pol})}$. For the polarizable solvent, $\alpha_\infty^{(\mathrm{pol})}$ is non-zero and $\alpha_0^{(\mathrm{pol})} < \alpha_{\mathrm{tot}}^{(\mathrm{pol})}$. Since the reorganization energy depends on the value of α_0, the polarizable and non-polarizable solvents have different reorganization energies. The ratio of reorganization energies is

$$\frac{\lambda^{(\mathrm{pol})}}{\lambda^{(\text{non-pol})}} = \frac{\alpha_0^{(\mathrm{pol})}}{\alpha_0^{(\text{non-pol})}} = 1 - \frac{\alpha_\infty^{(\mathrm{pol})}}{\alpha_{\mathrm{tot}}} = 1 - \frac{f_n(\epsilon_\infty)}{f_n(\epsilon_0)}. \tag{21}$$

This equation reflects that a mean field parameterization for a non-polarizable model of a polarizable solvent implicitly includes the contribution of electronic polarizability in order to produce accurate results for equilibrium solvation, $\alpha_0^{(\text{non-pol})} = \alpha_0^{(\mathrm{pol})} + \alpha_\infty^{(\mathrm{pol})}$. Thus $\alpha_0^{(\text{non-pol})}$ is parameterized for a non-polarizable solvent to include the effects of electronic polarizability. As a result, when a reorganization energy is predicted using a non-polarizable solvent model, it implicitly and incorrectly includes a contribution from the high frequency polarization modes.

The factor $\lambda^{(\mathrm{pol})}/\lambda^{(\text{non-pol})}$ is presented in Table I for the TIP4P-FQ model of water. The ratio $\lambda^{(\mathrm{pol})}/\lambda^{(\text{non-pol})}$ depends on the values of the static and optical dielectric constant of

TABLE I. The factor $\lambda^{(\mathrm{pol})}/\lambda^{(\mathrm{non\text{-}pol})}$ for TIP4P-FQ water is calculated using $\epsilon_0=80$ and $\epsilon_\infty=1.59$.

Solute	$\lambda^{(\mathrm{pol})}/\lambda^{(\mathrm{non\text{-}pol})}$
Monopole	0.62
Dipole	0.71

the solvent. We have used values appropriate for the TIP4P-FQ model in constructing Table I, $\epsilon_0=80$ and $\epsilon_\infty=1.59$. The ratio also depends on whether the electrostatic moment that is changing in the solute is a monopole, a dipole, a quadrupole, etc.; these relationships are described for monopole solvation in Eq. 7 and for dipole solvation in Eq. 8. We have reported results for both monopole and dipole solvation in Table I. The relationships assume that the radius of the solvent cavity is identical for the ground state and the excited state of the solute molecule. This assumption, which can lead to significant error, is discussed in Sec. II E.

In the context of electron transfer reactions, $\alpha_0^{(\mathrm{pol})}/\alpha_{\mathrm{tot}}$ is termed the Pekar factor. It is used to rescale the reorganization energy λ between a reactant state, DA, and a product state, D^+A^- (D signifies donor and A acceptor) to account for solvent polarizability. According to Marcus theory, the activation energy for an electron transfer reaction (ignoring quantum effects due to solvent librations and vibrations) is

$$E_{\mathrm{act}}=(\Delta G+\lambda)^2/4\lambda, \tag{22}$$

where $\Delta G=G_{D^+A^-}-G_{DA}$.[3,4] Rescaling the reorganization energy changes the height of the activation barrier. For long-range electron transfer, in which a charge is transferred over a distance of a several Å's, the factor for monopole solvation is often used. The value of this factor is 0.62 for reactions in TIP4P-FQ water.

In the simplified model we have been describing, the charges are taken to be at the centers of spherical cavities, and the polarization induced by one redox site on the solvent cavity around the other the redox site is neglected. More sophisticated treatments which address these restrictions produce correspondingly more complicated expressions for the Pekar factor.[53] The precise value of the Pekar factor depends on the solute and solvent geometry, but it is independent of the magnitude of the charge transfer between donor and acceptor. This constancy of the Pekar factor is simply a manifestation of the linear response inherent in a dielectric continuum formulation for the solvent.

The formaldehyde $^1A_1\rightarrow{}^1A_2$ transition results in a change of the dipole moment of the formaldehyde molecule. The dielectric continuum theory developed here indicates that the solvent reorganization energy for the transition should be a factor of 0.71 smaller in polarizable TIP4P-FQ water than in non-polarizable TIP4P water.

We note from the values in Table I that as the electrostatic moment changes from monopole to dipole, the ratio of reorganization energies in polarizable and non-polarizable solvents becomes closer to 1. For electronic transitions involving higher multipoles, the ratio will become even closer to 1. We assume that the lowest non-vanishing term in the multipole expansion for the electrostatic potential outside the solute will have the dominant effect on determining the reorganization energy. We therefore use the dipole result to analyze formaldehyde solvation.

E. Introducing non-linearity in the solute–solvent coupling

Although the linear coupling model expressed in Eq. 2 should explain most of the solute–solvent interactions, higher order, non-linear effects are also possible. An important source of non-linearity is the difference between the effective radius of the solute in the ground state and the excited state. In a study of the hydration of water, Rick and Berne found that it was necessary to use a charge-dependent radius in a continuum model to obtain good agreement with simulation results.[27] Similar non-linear effects due to dielectric saturation and electrostriction were observed in a study of the solvation of spherical cations.[54]

In another context, Chandler has shown that the non-linear coupling describing the exclusion of solvent from a spherical solute cavity yields the Percus–Yevick equation if the solvent fluctuations are Gaussian.[55–57] Excluding the solvent from the region of space occupied by the solute has the effect of renormalizing the solvent fluctuations (see Eq. 4.1 of Ref. 57):

$$\chi(r_1,r_2)=\chi_b(r_1,r_2)-\int_{\mathrm{in}}dr\int_{\mathrm{in}}dr'\chi_b(r_1,r)\chi_{\mathrm{in}}^{-1}(r,r')\chi_b(r',r_2). \tag{23}$$

In this equation, r_1 and r_2 are any two positions in the fluid, the fluctuations in solvent density in the presence of a solute are

$$\langle\delta\rho(r)\,\delta\rho(r')\rangle=\chi(r,r'), \tag{24}$$

the fluctuations in the bulk solvent are $\chi_b(r,r')$, and $\chi_{\mathrm{in}}^{-1}(r,r')$ is the functional inverse of $\chi_b(r,r')$ in the interior volume "in" of the solute. Since both χ and χ_{in}^{-1} are by necessity positive definite, the solvent fluctuations in the presence of the solute are strictly less than the fluctuations with no solute, i.e.

$$\mathrm{Tr}[\chi]-\mathrm{Tr}[\chi_b]=-\mathrm{Tr}[\chi_b\chi_{\mathrm{in}}^{-1}\chi_b]\leqslant 0. \tag{25}$$

The equality holds only if the interior region vanishes and the solute disappears. The renormalization of χ is equivalent to modifying the force constants α_∞ and α_0 in our model, resetting the scales for the fluctuations of the solvent polarization modes.

We proceed by describing a distinct radius for each solute state. For a spherical solute, the cavity radius can be defined from a thermodynamical perspective by using a Born-type formula. For example, for a spherical ion, the radius can be related to the mean potential at the solute due to the solvent, which in turn can be obtained from solute-solvent radial distribution functions.[58] A second method re-

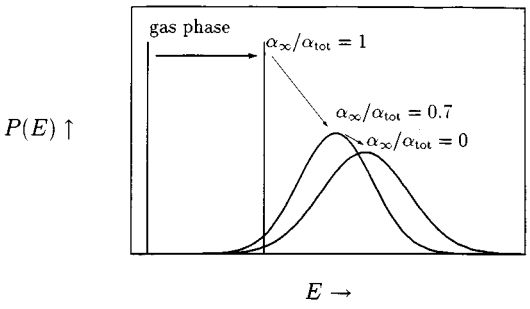

FIG. 2. The electronic absorption line shape of a solute changes as a function of the solvent polarizability. The gas phase line is assumed to be a delta function. In a solvent with purely electronic polarizability, the line shape remains a delta function but is shifted from the gas phase line. If the solvent polarization is due to slow orientational modes, the line shifts further and acquires a width.

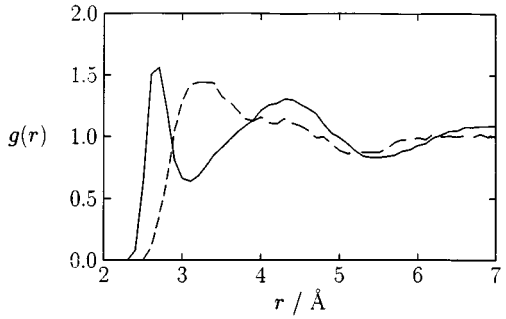

FIG. 3. The radial distribution function $g(r)$ is shown for the distance r between the oxygen site of formaldehyde and the oxygen site of water molecules in the solvent. The $g(r)$ for ground state formaldehyde is the solid line, and the $g(r)$ for excited state formaldehyde is the dashed line. The position of the first maximum in $g(r)$ is representative of the effective cavity size for each electronic state of the solute.

lates the radius to the fluctuations in the electric potential at the solute.[59] This method leads to a concise approximation,

$$1/R = \int_0^\infty dr\ g(r)/r^2, \tag{26}$$

where R is the effective radius and $g(r)$ is the radial distribution function between a spherical solute and a spherical, dipolar solvent; a similar formula can be obtained for a dipolar solute in a dipolar solvent.[59]

For the non-spherical formaldehyde solute, the cavity radius has been defined here as the first maximum in the radial distribution function $g(r)$ between the oxygen site of the formaldehyde and the oxygen sites of water molecules. The radial distribution function is defined by

$$N(r) = 4\pi r^2 \rho g(r)\, \delta r, \tag{27}$$

where ρ is the bulk number density of water molecules and $N(r)$ is the number of oxygen sites in a spherical shell of radius r and thickness δr centered on the oxygen of formaldehyde. Distribution functions from simulations of the ground state and the excited state of formaldehyde in polarizable TIP4P-FQ water are shown in Fig. 3. Correlations for the other solvents are similar and will be reported elsewhere.[58] From these correlations, we find that $R_1 = 2.65$ Å and $R_2 = 3.25$ Å.

The method we have used to determine R_1 and R_2 is certainly not unique. Indeed, it is unclear that a precise value can be assigned to the cavity radius for anything other than a hard sphere solute. Our choice has the virtue of being related directly to the solvation structure. It would not be correct, for instance, to equate the values of R_1 and R_2 with the Lennard-Jones radii for the ground and excited states: in our model the Lennard-Jones radii do not change (electrostriction in response to different solute charges causes the change in the cavity radius), nor are Lennard-Jones radii necessarily representative of the excluded volume of the solute.

The fluctuations of $\mathscr{E}_0$ and $\mathscr{E}_\infty$, characterized by α_0 and α_∞, can be related to the size of the solute cavity. Such a relationship between cavity size and the parameters α_0 and α_∞ is provided by Eqs. 7 and 8. We proceed by allowing each solute state to have its own effective radius, and by using these distinct radii to obtain the parameters α_0 and α_∞ appropriate for each solute state.

Let R_1 be the effective radius of the solute in electronic state 1. The corresponding solvent polarizabilities are $\alpha_0^{(1)}$ and $\alpha_\infty^{(1)}$. Similarly, the effective cavity radius for solute state 2 is termed R_2, and the corresponding polarizabilities are $\alpha_0^{(2)}$ and $\alpha_\infty^{(2)}$. According to Eq. 10, the solvent polarizabilities for each electronic state can be related very simply to the solute radii:

$$\alpha_\infty^{(i)} = R_i^{-(2n-1)} f_n(\epsilon_\infty),$$

and

$$\alpha_0^{(i)} = R_i^{-(2n-1)} [f_n(\epsilon_0) - f_n(\epsilon_\infty)],$$

where the function $f_n(\epsilon)$ is given in Eq. 9. The exponent $n=1$ for monopole solvation and $n=2$ for dipole solvation. According to these equations, if $R_2 > R_1$, then $\alpha_0^{(2)} < \alpha_0^{(1)}$ and $\alpha_\infty^{(2)} < \alpha_\infty^{(1)}$. This implies that solvent fluctuations are larger for smaller cavity sizes, in accord with the generic prediction of Eq. 25.

The effective solvent frequencies ω_0 and ω_∞ can also depend on the cavity size. Thus we introduce the solvent frequencies $\omega_0^{(1)}$ and $\omega_\infty^{(1)}$ for first solute electronic state and the frequencies $\omega_0^{(2)}$ and $\omega_\infty^{(2)}$ for the second electronic state.

The diabatic Hamiltonians of Eq. 3 are now

$$H_i = E_i + \frac{1}{2}\hbar\omega_\infty^{(i)} - \frac{1}{2}\alpha_\infty^{(i)} Q_i^2 + \frac{1}{2\alpha_0^{(i)}}\mathscr{E}_0^2 - \mathscr{E}_0 \cdot Q_i + \frac{1}{2}\alpha_0^{(i)}\omega_0^{(i)2}\Pi_0^2 \tag{28}$$

for $i=1$ and 2. Unlike Eq. 3, we have explicitly included the zero-point energy of the mode $\mathscr{E}_\infty$ as part of the diabatic Hamiltonian H_i. This is because the zero-point energy depends on the solute electronic state—each cavity size defines its own set of solvent normal modes. The free energy of solvation for species i is

$$\Delta G_i=\frac{1}{2}\hbar\omega_\infty^{(i)}-\frac{1}{2}[\alpha_0^{(i)}+\alpha_\infty^{(i)}]Q_i^2 \tag{29}$$

as calculated from Eq. 4.

The free energy difference ΔG_{21} can be calculated from the definition in Eq. 16,

$$\Delta G_{21}=\frac{1}{2}(\hbar\omega_\infty^{(2)}-\hbar\omega_\infty^{(1)})+k_BT\ln(\omega_0^{(2)}/\omega_0^{(1)}) -\frac{1}{2}[(\alpha_0^{(2)}+\alpha_\infty^{(2)})Q_2^2-(\alpha_0^{(1)}+\alpha_\infty^{(1)})Q_1^2]+(E_2-E_1). \tag{30}$$

The shift of the frequencies of the solvent modes is a nonlinear effect which contributes to the free energy difference ΔG_{21}.

The vertical excitation energy ΔE_{21} can be calculated from Eq. 11. At the moment of the excitation from state 1 to state 2, the solvent cavity is characteristic of electronic state 1. Thus it seems appropriate to use the bath parameters corresponding to state 1 when calculating the excitation energy ΔE_{21}. The bath parameters only reach the values characteristic of solute state 2 when solvation cage has relaxed, which takes place on the timescale of molecular translation. Note, therefore, that the vertical energy difference is not simply H_2-H_1, because H_2 represents the Hamiltonian for cavity size 2 rather than for cavity size 1. Instead, the vertical energy difference is $H_1(Q_2)-H_1(Q_1)$, where $H_1(Q_1)$ is H_1 as before, and $H_1(Q_2)$ is H_1 with Q_1 replaced with the new charges Q_2. This time lag in the parameters of the Hamiltonian should be correct because our entire solute–solvent coupling is electrostatic in nature. If we included a parameter in the Hamiltonian to represent non-electrostatic interactions, such as Van der Waals terms dependent on the solute electronic state, then we might expect the parameters representing these interactions to change instantaneously, and the energy difference H_2-H_1 might be more appropriate.

Bearing the above discussion in mind, we find that the vertical excitation energy is

$$\Delta E_{21}=-\frac{1}{2}\alpha_\infty^{(1)}(Q_2^2-Q_1^2)+\langle-\mathscr{E}_0\cdot(Q_2-Q_1)\rangle_1+E_2-E_1 =-\frac{1}{2}\alpha_\infty^{(1)}(Q_2^2-Q_1^2)-\alpha_0^{(1)}Q_1\cdot(Q_2-Q_1)+E_2-E_1. \tag{31}$$

The average $\langle\cdots\rangle_i$ is defined as

$$\langle\cdots\rangle_i\equiv\frac{\mathrm{Tr}_{\mathscr{E}_0}e^{-\beta H_i}(\cdots)}{\mathrm{Tr}_{\mathscr{E}_0}e^{-\beta H_i}} \tag{32}$$

for electronic state $i=1$ or 2. Similarly, the vertical energy for the reverse transition is

$$\Delta E_{12}=-\frac{1}{2}\alpha_\infty^{(2)}(Q_1^2-Q_2^2)-\alpha_0^{(2)}Q_2\cdot(Q_1-Q_2) +E_1-E_2. \tag{33}$$

In Eq. 18, the reorganization energy λ was defined as the energy difference $\Delta E_{21}-\Delta G_{21}$. Furthermore, λ was also given by the symmetrical difference $\Delta E_{12}-\Delta G_{12}$. This definition of the reorganization energy produces different values of λ for each transition:

$$\lambda^{(1)}\equiv\Delta E_{21}-\Delta G_{21} =\frac{1}{2}\alpha_0^{(1)}(Q_1-Q_2)^2-\frac{1}{2}(\alpha_0^{(1)}+\alpha_\infty^{(1)}-\alpha_0^{(2)}-\alpha_\infty^{(2)})Q_2^2 +\frac{1}{2}(\hbar\omega_\infty^{(1)}-\hbar\omega_\infty^{(2)})+k_BT\ln(\omega_0^{(1)}/\omega_0^{(2)});$$

$$\lambda^{(2)}\equiv\Delta E_{12}-\Delta G_{12} =\frac{1}{2}\alpha_0^{(2)}(Q_1-Q_2)^2-\frac{1}{2}(\alpha_0^{(2)}+\alpha_\infty^{(2)}-\alpha_0^{(1)}-\alpha_\infty^{(1)})Q_1^2 +\frac{1}{2}(\hbar\omega_\infty^{(2)}-\hbar\omega_\infty^{(1)})+k_BT\ln(\omega_0^{(2)}/\omega_0^{(1)}). \tag{34}$$

The absorption line shape, $P_{2\leftarrow1}(E)$, and the fluorescence line shape, $P_{1\leftarrow2}(E)$, have different widths. Each line shape remains a Gaussian, however:

$$P_{2\leftarrow1}(E)=[2\pi k_BT\alpha_0^{(1)}(Q_2-Q_1)^2]^{-1/2} \times\exp[-(E-\Delta E_{21})^2/2k_BT\alpha_0^{(1)}(Q_2-Q_1)^2];$$

$$P_{1\leftarrow2}(E)=[2\pi k_BT\alpha_0^{(2)}(Q_2-Q_1)^2]^{-1/2} \times\exp[-(E-\Delta E_{12})^2/2k_BT\alpha_0^{(2)}(Q_2-Q_1)^2].$$

Thus, the widths of the absorption and fluorescence lines, which we define as $\sigma_0^{(1)}$ and $\sigma_0^{(2)}$, are given from the spectral line shapes as

$$\sigma_0^{(1)}=\sqrt{k_BT\alpha_0^{(1)}}|Q_2-Q_1|; \tag{35a}$$

$$\sigma_0^{(2)}=\sqrt{k_BT\alpha_0^{(2)}}|Q_2-Q_1|. \tag{35b}$$

These equations, simply the generalization of Eq. 13 to different size cavities, indicate that the relative width of the fluorescence spectrum to the absorption spectrum should be $\sqrt{\alpha_0^{(2)}/\alpha_0^{(1)}}$. Thus, a change in relative widths of the fluorescence and absorption line shapes signals a non-linear coupling between the solute and solvent.

A symmetrized form of λ, which we term λ_+, can be defined:

$$\lambda_+\equiv\frac{1}{2}(\Delta E_{12}+\Delta E_{21}) =\frac{1}{2}(\lambda^{(1)}+\lambda^{(2)}) =\frac{1}{4}(\alpha_0^{(1)}+\alpha_0^{(2)})(Q_1-Q_2)^2+\frac{1}{4}(\alpha_{\mathrm{tot}}^{(1)}-\alpha_{\mathrm{tot}}^{(2)})(Q_1^2-Q_2^2). \tag{36}$$

The definition of λ_+ corresponds to the operational definition we used to extract reorganization energies from our computer simulations.

Now we concentrate on the quantity λ_+. We imagine two solvents, one polarizable, i.e. α_∞ is non-zero, and the other non-polarizable in the sense that α'_∞ for that solvent is zero. (Quantities corresponding to the non-polarizable solvent are primed ($'$) and quantities corresponding to the polarizable solvent are unprimed.) We assume that the two solvents have the same total polarizability, $\alpha_0+\alpha_\infty=\alpha'_0+\alpha'_\infty$. We wish to calculate the ratio λ_+/λ'_+. To simplify our evaluation of this ratio, we write $\lambda_+=A+B$ and $\lambda'_+=A'+B'$, where

$$A=\frac{1}{4}(\alpha_0^{(1)}+\alpha_0^{(2)})(Q_1-Q_2)^2,$$

$$A'=\frac{1}{4}(\alpha_0^{(1)\prime}+\alpha_0^{(2)\prime})(Q_1-Q_2)^2,$$

$$B=\frac{1}{4}(\alpha_{\rm tot}^{(1)}-\alpha_{\rm tot}^{(2)})(Q_1^2-Q_2^2),$$

and

$$B'=\tfrac{1}{4}(\alpha_{\rm tot}^{(1)\prime}-\alpha_{\rm tot}^{(2)\prime})(Q_1^2-Q_2^2).$$

In these equations, $\alpha_{\rm tot}^{(i)}=\alpha_0^{(i)}+\alpha_\infty^{(i)}$ for $i=1$ and 2, and likewise $\alpha_{\rm tot}^{(i)\prime}=\alpha_0^{(i)\prime}+\alpha_\infty^{(i)\prime}$. Furthermore, our assumption that the two solvents have the same total polarizability implies that $B'=B$. We find that

$$\frac{\lambda_+}{\lambda'_+}=\frac{\rho_+[1-f_n(\epsilon_\infty)/f_n(\epsilon_0)](Q_1-Q_2)+\rho_-(Q_1+Q_2)}{\rho_+(Q_1-Q_2)+\rho_-(Q_1+Q_2)}, \tag{37}$$

where $\rho_\pm=R_1^{-(2n-1)}\pm R_2^{-(2n-1)}$, and $n=1$ for monopole solvation and 2 for dipole solvation.

First we note that if there is no change in the cavity radius, then $\rho_-=0$ and $\lambda_+/\lambda'_+=1-f_n(\epsilon_\infty)/f_n(\epsilon_0)$. The polarizable TIP4P-FQ model of water has $\epsilon_0=80$ and $\epsilon_\infty=1.592$, implying for dipole solvation that $f_2(\epsilon_0)=0.98$ and $f_2(\epsilon_\infty)=0.28$. As before, the ratio $\lambda_+/\lambda'_+=0.71$.

Using $R_1=2.65$ Å and $R_2=3.25$ Å, as well as the parameters $Q_1=3.97$ D and $Q_2=2.49$ D consistent with the simulations, we find that λ_+/λ'_+ changes from 0.71 to 0.86. We see that the non-linear effects due to changes in the cavity size of the solute molecule reduce the differences between the reorganization energy measured in a polarizable versus a non-polarizable solvent.

It is also possible to define a quantity similar to ΔG_{21} which we term λ_-:

$$\lambda_-\equiv\frac{1}{2}(\Delta E_{21}-\Delta E_{12})$$

$$=\frac{1}{4}(\alpha_{\rm tot}^{(1)}+\alpha_{\rm tot}^{(2)})(Q_1^2-Q_2^2)+\frac{1}{4}(\alpha_0^{(1)}-\alpha_0^{(2)})(Q_1-Q_2)^2. \tag{38}$$

The quantity λ_- corresponds to our operational definition for obtaining ΔG_{21} from simulation results. We now investigate the extent to which changes in the cavity size affect the value of ΔG_{21} measured in polarizable versus non-polarizable solvents.

TABLE II. Parameters and properties are shown for three water models: non-polarizable TIP4P, non-polarizable TIP4P-MQ, and polarizable TIP4P-FQ.

	Water model		
	TIP4P	TIP4P-MQ	TIP4P-FQ[a]
Parameter			
$R_{\rm OH}$ (Å)	0.9572	0.9572	0.9572
$R_{\rm OM}$ (Å)	0.15	0.15	0.15
∠HOH (degrees)	104.52	104.52	104.52
$\sigma_{\rm LJ}$ (Å)	3.154	3.159	3.159
$\epsilon_{\rm LJ}$ (kcal/mol)	0.1550	0.2862	0.2862
μ (D)	2.18	2.625	2.625[b]
$Q_{\rm H}$ ($\lvert e\rvert$)	0.52	0.627	0.619[i]
Property			
ϵ_0[c]	53 ± 2[d]		79 ± 8
ϵ_∞[e]	1	1	1.592 ± 0.003
Diffusion constant[f] (10^{-5}cm^2/sec)	3.6 ± 0.2[g]	6.0 ± 0.1	1.9 ± 0.1
$\tau_{\rm NMR}$[h] (ps)	1.4 ± 0.2[g]	7.3 ± 0.2	2.1 ± 0.1

[a]From Ref. 39.
[b]The thermal average $\langle\lvert\mu\rvert\rangle$ is reported for bulk TIP4P-FQ water. The average dipole projected along the C_{2V} axis is 2.59 D.
[c]The experimental value is 78 (Ref. 81).
[d]From Ref. 61.
[e]The experimental value is 1.79 (Ref. 81).
[f]The experimental value is 2.3×10^{-5}cm^2/s (Ref. 82).
[g]From Ref. 84.
[h]The experimental value is 2.1 ps (Ref. 83).
[i]The thermal average $\langle Q_{\rm H}\rangle$ is reported for bulk TIP4P-FQ water.

To estimate these non-linear effects, we calculate the ratio λ_-/λ'_-, where the $'$ again signifies a quantity measured in a non-polarizable solvent with $\epsilon'_\infty=1$. We find that

$$\frac{\lambda_-}{\lambda'_-}=\frac{\rho_+(Q_1+Q_2)+\rho_-[1-f_n(\epsilon_\infty)/f_n(\epsilon_0)](Q_1-Q_2)}{\rho_+(Q_1+Q_2)+\rho_-(Q_1-Q_2)}. \tag{39}$$

With the previous choices for the quantities which appear in this expression, we find that the ratio $\lambda_-/\lambda'_-=0.98$. We conclude that the value for ΔG_{21} obtained in a simulation using a polarizable solvent should be indistinguishable from the value of ΔG_{21} obtained using a non-polarizable solvent. This can occur even if the solute radii are substantially different in each state.

III. MODEL

A. Water

Four treatments of water were used in simulations. The parameters for the water models are presented in Table II. The first model, TIP4P, is a standard non-polarizable model for water.[40] It has a static dipole moment of 2.18 D and a dielectric constant of 53 ± 2.[61] This model has charge interactions on the hydrogen sites and on a site known as the M site displaced 0.15 Å from the oxygen site. There is also a Lennard-Jones interaction between oxygen sites.

The polarizable model we use is the fluctuating charge model, TIP4P-FQ.[39] This model shares the rigid geometry of the TIP4P model. Instead of having fixed charges, however,

TABLE III. Lennard-Jones parameters for formaldehyde.

Site	σ (Å)	ϵ (kcal/mol)
O	2.85	0.20
C	3.296	0.12
H	2.744	0.01

TABLE IV. Charge set for formaldehyde.

		Charges ($\|e\|$)		
Electronic state	μ (D)	O	C	H
$^1A_1$	3.97	−0.577	0.331	0.123
$^1A_2$	2.49	−0.280	−0.040	0.160

the charges on the FQ molecule are allowed to redistribute in response to the local electrostatic environment. Thus an isolated FQ water molecule has a dipole moment of 1.85 D, characteristic of the gas phase, while in the bulk the molecules polarize each other and the mean dipole moment increases to 2.625 D. The parameters for the Lennard-Jones interactions for the FQ model differ slightly from the parameters for TIP4P water. The FQ model has a dielectric constant of 79 ± 8.[39]

The MQ model is a non-polarizable model identical to the FQ model, except that the charges on the interaction sites are held fixed. The charges were obtained by requiring the permanent dipole moment on an MQ water molecule to be the same as the mean dipole moment on an FQ water molecule in bulk water, $\langle|\mu|\rangle=2.625$ D. This corresponds to a hydrogen charge of $0.627|e|$. Another method for obtaining a fixed-charge analog for the FQ model is to choose fixed charges to yield the same permanent dipole as the mean dipole along the C_{2V} axis of a bulk FQ water, $\langle\mu_z\rangle=$ 2.59 D. However, the difference between this method and the method we used is very small and changes the charges by only about 1%.

Differences between the FQ and MQ models can arise from at least two sources: 1) the FQ and MQ models can produce different solvent configurations; 2) for the same solvent configuration, the FQ and MQ models can produce different results because the FQ solvent is polarizable and the MQ solvent is non-polarizable. In order to discriminate between these two possible sources of differences, we performed simulations with a hybrid solvent we termed FQ/MQ. For this solvent, the solvent configurations are taken from a simulation employing FQ water, i.e. the configurations are consistent with a polarizable model for water. However, the fixed MQ charges are employed when absorption and fluorescence energies are calculated. Thus, differences between the FQ and FQ/MQ models are due solely to the effects of polarizability because the solvent structures for the two models are identical.

B. Formaldehyde

We have based our model for formaldehyde on a model developed by Levy and coworkers.[41–43] The fixed geometry has $R_{CO}=1.184$ Å, $R_{CH}=1.093$ Å, and $\angle HCH=115.5°$. The Lennard-Jones parameters for formaldehyde, which we have adopted from Ref. 43, are listed in Table III. These parameters are standard literature values.[62] Identical Lennard-Jones parameters were used for the ground and excited states of formaldehyde. Combining rules were used to obtain the Lennard-Jones interactions between the formaldehyde sites and the oxygen site on water: $\sigma=(\sigma_1+\sigma_2)/2$ and $\epsilon=\sqrt{\epsilon_1\epsilon_2}$. Because the Lennard-Jones parameters for TIP4P water differ from the parameters for FQ (and MQ) water, the Lennard-Jones interactions between a TIP4P water and formaldehyde differ from the interactions between an FQ water and formaldehyde. It might have been more appropriate to use the same Lennard-Jones interactions rather than to use combining rules. Previous studies of hydrophobic hydration of methane in polarizable and non-polarizable water have shown that the difference in Lennard-Jones interactions can have a significant effect.[38,63] These effects due to Lennard-Jones interactions, observed in the solvation of non-polar, hydrophobic molecules such as methane, might not be as significant in solvation of a polar molecule like formaldehyde.

We employed a charges set introduced by Levy and coworkers.[41] These charges produce a ground state dipole of 3.97 D and an excited state of 2.49 D. The charges, listed in Table IV, are much too large for a realistic model of formaldehyde. The gas phase dipole moments are known from experiment to be 2.3 D (Refs. 64, 65) and 1.57 D.[66,67] As we discuss elsewhere, *ab initio* calculations suggest that the ground and excited state dipole moments of formaldehyde in water are enhanced to 2.91 D and 1.88 D.[29] When this set of *ab initio* charges is used,[29] or when *ab initio* methods are used to calculate the transition energy directly,[41] the agreement with the experimental absorption spectrum is quite good.

C. Simulation method

We performed simulations to probe the solvent-induced frequency shift of the electronic transition between the formaldehyde ground state and the formaldehyde excited state. The system simulated consisted of a periodically replicated box 18.6 Å on a side containing 209 water molecules and a single formaldehyde molecule. A timestep of 1 fs was used, and the solvent and solute molecules were kept rigid using the algorithm RATTLE.[68–70] Ewald sums were used to evaluate the electrostatic interactions. We have checked for finite size effects by measuring the contribution of solvent molecules to the vertical transition energy for the formaldehyde solute as a function of the distance between the solute and solvent molecules. We find that water molecules beyond 7.5 Å make virtually no contribution to the energy of the vertical transition, indicating that our results are converged with respect to system size.

In the simulations employing the non-polarizable TIP4P and MQ models of liquid water, the solvent shift for the

electronic transition was calculated as follows. The electrostatic interactions between the solvent molecules and the ground and excited states of the solute are

$$V_0 = V_{\mathrm{LJ}} + V_{\mathrm{WW}} + \sum_\alpha Q_\alpha^0 \sum_i Q_i / |R_\alpha - R_i|, \tag{40a}$$

$$V^* = V_{\mathrm{LJ}} + V_{\mathrm{WW}} + \sum_\alpha Q_\alpha^* \sum_i Q_i / |R_\alpha - R_i|. \tag{40b}$$

The term V_{LJ} contains the solute–solvent and solvent–solvent Lennard-Jones interactions, and the term V_{WW} contains the electrostatic interactions between different water molecules. The index α runs over the formaldehyde sites, Q_α^0 is the ground state charge for site α, and Q_α^* is the excited state charge. The index i runs over charge sites on all of the water molecules. The difference in energy for the vertical transition is $V^* - V_0$. Both V_{LJ} and V_{WW} are unchanged during the transition and drop out of $V^* - V_0$.

The solvent shift for the electronic transition in the polarizable FQ solvent is slightly more complicated to calculate. The part of the potential energy due to charge interactions between water molecules is different for each of the electronic states of the solute because the ground and excited state solute charge distributions induce different charges on the polarizable solvent molecules. The ground state and excited state energies are

$$V_0 = V_{\mathrm{LJ}} + V_{\mathrm{pol}}^0 + V_{\mathrm{WW}}^0 + \sum_\alpha Q_\alpha^0 \sum_i Q_i^0 / |R_\alpha - R_i|, \tag{41a}$$

$$V^* = V_{\mathrm{LJ}} + V_{\mathrm{pol}}^* + V_{\mathrm{WW}}^* + \sum_\alpha Q_\alpha^* \sum_i Q_i^* / |R_\alpha - R_i|, \tag{40b}$$

where $\{Q_i^0\}$ are the water charges in the ground state and $\{Q_i^*\}$ are the water charges in the excited state. The polarization self-energy for the ground state charges is V_{pol}^0, and the polarization self-energy for the excited state charges is V_{pol}^*. The water–water interactions in V_{WW}^0 are determined using the set of charges $\{Q_i^0\}$, and the water–water interactions in V_{WW}^* are determined using the set of charges $\{Q_i^*\}$. Thus, in addition to the direct solute–solvent interactions, the energy differences $V_{\mathrm{pol}}^* - V_{\mathrm{pol}}^0$ and $V_{\mathrm{WW}}^* - V_{\mathrm{WW}}^0$ also contribute to the vertical energy difference $V^* - V_0$ for a polarizable solvent. The Lennard-Jones interactions V_{LJ} are the same for each state and do not contribute to the energy difference.

We focus attention now on differences between the energy gap ΔE_{21} measured in a non-polarizable solvent (such as TIP4P or MQ) and in a polarizable solvent (such as FQ). One source contributing to differences is that the solvation structures generated using a polarizable solvent model might differ from those generated using a non-polarizable solvent.

As we mentioned in Sec. III A, a second source of differences between the results for polarizable and non-polarizable solvent models is that the charges induced on a polarizable solvent molecule by the formaldehyde solute will deviate from the charges induced on a water molecule in the bulk. To reiterate, we focused on this second contribution to differences by performing a set of simulations which we have termed FQ/MQ. In this set of simulations, we obtained fixed molecular configurations using the polarizable FQ water model. To calculate the energy gap, however, we replaced the polarizable FQ charges with the fixed MQ charges and then used Eq. 40. In this respect we can discriminate to changes to the solvation energy due solely to the induced charges and changes due to differences in the solvation structure itself.

When performing the simulations for each of the charge sets and each of the solvents, we used at least 40 ps. Data collection lasted 100 ps.

The simulations were all performed on a 16 node partition of a CM5 from Thinking Machines Corporation. For a system consisting of 216 water molecules, each simulation step took approximately 0.3 CPU seconds. When the formaldehyde molecule was added, the CPU time per step increased to 0.5 CPU seconds. The marked increase in computer time is a consequence of the parallel nature of the molecular dynamics algorithm we employed and the architecture of the CM5. Much of the increase in the time per step reflects overhead required for the calculation of solute–solvent interactions. This overhead should be almost independent of the number of solute molecules. Therefore, we suspect that the CPU time per step would remain close to 0.5 seconds even if we added many more solute molecules.

In comparing the CM5 timings to timings on other computers, it is important to note that our implementation for a single solute molecule has not been optimized for the parallel architecture. The simulation of pure solvent, which requires 0.3 CPU seconds per step, has been optimized. On an IBM 370, a single step of molecular dynamics for 216 TIP4P-FQ water molecules requires 1.5 CPU seconds. This comparison for our code indicates that a 16 node partition of a CM5 is equivalent to 5 IBM 370's.

IV. RESULTS AND DISCUSSION

Below, we present results for the absorption and fluorescence maxima, the widths of the spectral peaks, and the free energies and reorganization energies for the two electronic states of formaldehyde in the simulations. The gas-phase contributions E_1 and E_2 have been removed from the energies in order to focus entirely on solvent contributions.

A. Absorption line shapes

Absorption line shapes for the transition from the solute ground state to excited state are shown in Fig. 4. It is important to remember that, for a polarizable solvent, the solvent shift consists of a part due to the direct water–formaldehyde interactions and a part due to the change in water–water interactions which represents a many-body polarization energy. The water–water interactions are included when the total shift is calculated. Results are presented for four solvents: polarizable FQ (solid lines); non-polarizable FQ/MQ (dot-dash lines); non-polarizable MQ (dashed lines); and non-polarizable TIP4P (dotted lines). These lineshapes represents the solvent shift from the gas phase formaldehyde

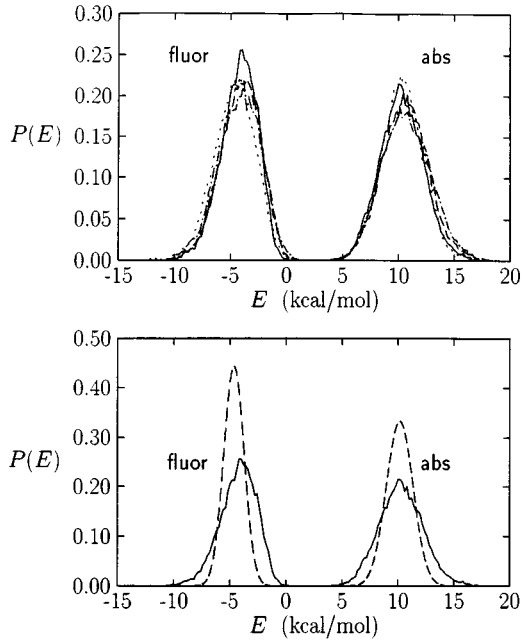

FIG. 4. Top panel: The absorption spectra for the solute transition 3.97 D $\rightarrow$ 2.49 D and the fluorescence spectra for the solute transition 2.49 D $\rightarrow$ 3.97 D are shown for four solvent models: FQ (solid); FQ/MQ (dot-dash); MQ (dashed); TIP4P (dotted). The absorption peak is near 10.5 kcal/mol and the fluorescence peak is near -4.3 kcal/mol. Bottom panel: The absorption and fluorescence spectra from the polarizable FQ solvent simulations (solid lines) are compared with theoretical predictions (dashed lines) based on non-polarizable simulation results ($\Delta G = 7.4$ kcal/mol, $\lambda = 3.2$ kcal/mol) and the cavity-radius-corrected ratio $\lambda^{(\mathrm{pol})}/\lambda^{(\mathrm{non\text{-}pol})} = 0.86$.

transition. All of the solvent models produce a similar absorption band with a maximum close to 10 kcal/mol (0.43 eV or 3500 cm^{-1}) and a root mean square width of 2 kcal/mol (0.087 eV or 700 cm^{-1}).

The non-polarizable FQ/MQ and MQ solvents have peaks which are at slightly higher energies than the polarizable FQ solvent, 10.6–10.7 kcal/mol versus 10.3 kcal/mol. The widths of the peaks are also slightly larger for the non-polarizable solvents, 2.1–2.2 kcal/mol for FQ/MQ and MQ versus 2.0 kcal/mol for FQ. These differences are consistent in general with the dielectric continuum theory. The peak for the TIP4P simulation is at 10.3 kcal/mol, and the width is 1.9 kcal/mol. Thus, there is general agreement between the results from simulations employing quite different models for water.

B. Fluorescence shifts

The fluorescence shifts for vertical transitions returning to the ground state surface from the excited state surface are shown in Fig. 4. Results are shown for four solvent models: FQ (solid lines); FQ/MQ (dot-dash); MQ (dashed); and TIP4P (dotted). The fluorescence energy is defined as $E^* - E_0$, where E^* is the energy on the initial (excited state) surface and E_0 is the energy on the final (ground state) surface following the vertical transition. The peaks for the polarizable FQ and non-polarizable FQ/MQ and MQ solvent models are all very close, roughly -4.3 kcal/mol (-0.19 eV or -1500 cm^{-1}). The peak for the TIP4P solvent is at -4.7 kcal/mol, slightly shifted from the other simulations.

The fluorescence shifts are smaller than the absorption shifts because the water molecules are less ordered around the less polar excited state solutes. The widths of the fluorescence peaks are smaller than the widths of the absorption peaks by about 0.3 kcal/mol. The only exception is the width of the peak for TIP4P water, which is only 0.1 kcal/mol smaller than the width of the absorption line. In comparison, the experimental line width is close to 4400 cm^{-1} or 12–13 kcal/mol, although *ab initio* studies indicate that much of the broadening is due intramolecular distortion of the solute and the solvent contribution is only 1100 cm^{-1} or about 3 kcal/mol.[41]

As we will discuss below, the width of the peaks are related to the reorganization energy. A difference between the absorption and fluorescence peak widths indicates that a single reorganization energy cannot characterize the solvent response, and the free energy surfaces have different curvatures. Based on Sec. II E, this difference can be related to the difference in the effective radius of the solvent cavity for the ground state and the excited state solute. We can use Eq. 35 to predict that the ratio of the width of the fluorescence spectrum to the width of the absorption spectrum should scale as $(R_1/R_2)^{(2n-1)/2}$. In our case, with $R_1 = 2.65$ Å and $R_2 = 3.25$ Å, this ratio of widths is predicted to be 0.74. The ratio from the simulations is 0.8 for the FQ solvent, 0.86 for the FQ/MQ and MQ solvents, and 0.95 for the TIP4P solvent.

The line shape for the fluorescence is asymmetric with a skew toward solvent shifts which are more negative and larger in magnitude. The statistical uncertainties in the fluorescence spectra are indicated by the noise in Fig. 4. It is evident from the figure that the absolute error is relatively constant over the entire range of the spectra, and is quite small relative to the spectral widths. Thus the widths and centers of the spectra are known quite accurately, and the skew is indeed statistically significant. (If we were to compute the free energy surface near the wings, which requires taking the logarithm of the absorption spectra, the absolute error in the free energy would be proportional to the relative error of the absorption spectra. The relative error of an absorption spectrum is quite large at the wings, and umbrella sampling is required to obtain good statistics for the free energy.[71])

We attribute the skew in the spectral lines to interactions with water molecules that are very close to the formaldehyde. Occasionally, a water molecule will be very close to the formaldehyde molecule during the electronic transition and there will be a large contribution to the solvent shift. These infrequent conformations produce the skew in the line shape. The skew in the fluorescence spectra is larger than the skew in the absorption spectra. Presumably, the absorption line shape is more symmetric because, by the central limit theorem, independent contributions from many solvent molecules add to form a Gaussian line. In the fluorescence spectra, contributions from only a few water molecules are domi-

TABLE V. Table of energies, all in kcal/mol[a]

	Solvent Model			
	FQ	FQ/MQ	MQ	TIP4
ϵ_0	80	~80	~80	53
ϵ_∞	1.592	1	1	1
$\sigma_0^{(1)}$	2.0	2.2	2.1	1.9
$\sigma_0^{(2)}$	1.6	1.9	1.8	1.8
ΔE_{21}	10.3	10.7	10.6	10.3
ΔE_{12}	−4.3	−4.3	−4.2	−4.7
ΔG_{21}	7.3	7.5	7.4	7.5
λ from $(\Delta E_{12}+\Delta E_{21})/2$	3.0	3.2	3.2	2.8
λ from $(\sigma_0^{(1)})^2/2k_BT$	3.4	4.1	3.7	3.0
λ from $(\sigma_0^{(2)})^2/2k_BT$	2.2	3.0	2.7	2.7

[a]One standard deviation uncertainty is about ±0.1 kcal/mol for each of the reported energies.

nant, and lines are no longer Gaussian. Thus, the free energy surface is non-parabolic.

C. Free energies and reorganization energies

We report in Table V the results for the calculations of σ_0, ΔE_{21}, ΔE_{12}, ΔG_{21}, and λ for the four solvent models we have considered: FQ, FQ/MQ, MQ, and TIP4P. The reorganization energy λ is calculated in three different ways: first from the average of ΔE_{12} and ΔE_{21}, and again from the widths $\sigma_0^{(1)}$ and $\sigma_0^{(2)}$ of the absorption and fluorescence lines. We first describe the simulation results, starting with the solvent shift for the electronic transition from ground state to excited state, ΔE_{21}. The experimental shift for formaldehyde in water has not been measured because of oligomer formation. The experimental value for the shift for acetone in water is 1900 cm^{-1}, or 5.4 kcal/mol.[72] We find a solvent shift of about 10 kcal/mol from simulation. This agrees very well with the previous simulation results of Levy and coworkers,[41,43] but is almost twice as large as the shift measured experimentally for acetone. As mentioned in Sec. III B, the transition energy is too large because the solute charges are unrealistically large. When the charges are fit by electrostatic fitting one finds charges that give much better agreement with experiment.[60]

The solvent shift in the excited state fluorescence line, ΔE_{12}, is generally smaller in magnitude than the shift in the absorption line. This is because the excited state is less polar than the ground state and there is less order in the solvent. We also note that in the simulations there is little difference between the value of ΔE_{12} in the polarizable FQ solvent and the value of ΔE_{12} in the non-polarizable solvents. Also, little difference is seen in the values of ΔE_{21} in the polarizable and non-polarizable solvents. Furthermore, the values calculated for the solvation energy difference ΔG_{21} and the reorganization energy λ (being related to sums and differences of ΔE_{12} and ΔE_{21}) are nearly identical for the two solvents.

As expected, the equilibrium solvation free energy differences ΔG_{21} are similar for polarizable and non-polarizable solvents: ΔG_{21} depends only on the static dielectric constant, and the static dielectric constants of all the water models are similar. Furthermore, the change in the cavity size does not greatly affect ΔG_{21}.

It is surprising, however, that the values obtained for λ from the definition $\lambda=(\Delta E_{12}+\Delta E_{21})/2$ are similar for polarizable and non-polarizable solvent. For the FQ model, $\lambda=3.0$ kcal/mol, and for the MQ and FQ/MQ models, $\lambda=3.2$ kcal/mol. The high-frequency optical dielectric constants are different for the polarizable and non-polarizable models. Since the reorganization energy λ should depend on both the static and the optical dielectric constants, we would have expected that the reorganization energy λ was different in the different solvents. We see from Table I that the difference, expressed as the ratio $\lambda^{(\text{pol})}/\lambda^{(\text{non-pol})}$, should be a factor of 0.71 for FQ relative to MQ water. Accounting for changes in the size of the solute cavity yields a ratio of 0.86, as discussed in Sec. II E. Using the values $\lambda^{(\text{pol})}=3.0\pm0.1$ kcal/mol and $\lambda^{(\text{non-pol})}=3.2\pm0.1$ kcal/mol from the simulations, we obtain a ratio of 0.94 ± 0.05. The theoretical prediction lies just outside the one standard deviation error bounds of the simulation results.

We note finally that there is a self-consistency check to perform involving the reorganization energy λ and the linewidth σ_0, namely that λ can be obtained from the peak width σ_0 as $\sigma_0^2/2k_BT$. We have used the absorption linewidth $\sigma_0^{(1)}$ and the fluorescence linewidth $\sigma_0^{(2)}$ to compute values for λ. These values are also shown in Table V. The reorganization energies obtained from the linewidths bracket the values of λ calculated from $(\Delta E_{12}+\Delta E_{21})/2$, indicating that the peak widths are indeed consistent with the reorganization energy.

The peak widths for the TIP4P model are consistently smaller than the widths for the other non-polarizable models. This indicates that solvent fluctuations are smaller for TIP4P than for the other models and is consistent with TIP4P having the smallest dielectric constant of all the models.

Finally, we have used the simulation results for the non-polarizable FQ/MQ and MQ models to predict the absorption and fluorescence line shapes for the FQ solvent. The predicted lines are determined by four parameters: the peak centers ΔE_{21} and ΔE_{12} and the peak widths $\sigma_0^{(1)}$ and $\sigma_0^{(2)}$. We have obtained these parameters from the non-polarizable simulations as follows. We start with $\Delta G_{21}=7.4$ kcal/mol and $\lambda=3.2$ kcal/mol from the simulations with non-polarizable solvent. The free energy difference ΔG_{21} is used without any change, but λ is rescaled by the factor 0.86 derived in Sec. II E to subtract the contribution of the electronic polarization modes. The rescaled value of λ is 2.75 kcal/mol. The absorption peak center ΔE_{21} is $\lambda+\Delta G_{21}$, and the fluorescence peak center ΔE_{12} is $\lambda-\Delta G_{12}$. The widths of the spectral lines are determined from λ. We now describe four methods of estimating these widths.

The first method is appropriate when the solute cavity does not change its size, implying that the absorption and fluorescence lines have identical widths. In this case,

$$\sigma_0^{(1)}=\sigma_0^{(2)}=\sqrt{2k_BT\lambda}. \tag{42}$$

This method yields linewidths of 1.8 kcal/mol based on $\lambda = 2.75$ kcal/mol. The widths from this method are very close to the widths seen in the simulation.

In the second method, we account for the difference in the cavity sizes of the ground state and excited state by assuming $\sigma_0^{(2)}/\sigma_0^{(1)} = (R_1/R_2)^{3/2}$. (See Sec. II E for the reasoning behind this choice.) We rewrite Eq. 36 as

$$\lambda = [(\sigma_0^{(1)})^2 + (\sigma_0^{(2)})^2]/4k_BT + \frac{1}{4}(\alpha_{\rm tot}^{(1)} - \alpha_{\rm tot}^{(2)})(Q_1^2 - Q_2^2). \tag{43}$$

If the total polarizabilities $\alpha_{\rm tot}^{(1)}$ and $\alpha_{\rm tot}^{(2)}$ are similar, the second term on the right-hand-side of this equation can be ignored. In this case, we find that

$$\sigma_0^{(1)} = \sqrt{4k_BT\lambda/[1+(R_1/R_2)^3]}, \tag{44a}$$

and

$$\sigma_0^{(2)} = \sqrt{4k_BT\lambda/[1+(R_2/R_1)^3]}. \tag{44b}$$

This method predicts the widths $\sigma_0^{(1)} = 2.05$ kcal/mol and $\sigma_0^{(2)} = 1.5$ kcal/mol, which we used in constructing Fig. 4. The agreement with the simulation results is very good.

We note, however, that the above treatment is inconsistent because of the term in Eq. 43 that was ignored. We can include the term in Eq. 43 which involves the total polarizability $\alpha_{\rm tot}$ by using the relationship from Eq. 10 that $\alpha_{\rm tot}/\alpha_0 = f_n(\epsilon_0)/[f_n(\epsilon_0) - f_n(\epsilon_\infty]$, and again assuming that $\sigma_0^{(2)}/\sigma_0^{(1)} = (R_1/R_2)^{3/2}$. A bit of algebra yields

$$\sigma_0^{(1)} = \sqrt{4k_BT\lambda/\left\{1+(R_1/R_2)^3 + [1-(R_1/R_2)^3]\frac{f_n(\epsilon_0)}{f_n(\epsilon_0)-f_n(\epsilon_\infty)}\frac{Q_1+Q_2}{Q_1-Q_2}\right\}}. \tag{45}$$

Using the same values for $f_n(\epsilon_0)$ and $f_n(\epsilon_\infty)$ as in Sec. II E, we find that the widths are $\sigma_0^{(1)} = 1.2$ kcal/mol and $\sigma_0^{(2)} = 0.9$ kcal/mol, much narrower than the widths observed in the simulations.

The term in Eq. 43 involving the total polarization can be included by relating its value to that of ΔG_{21}. We rewrite Eq. 38 as

$$\Delta G_{21} = \frac{1}{4k_BT}[(\sigma_0^{(1)})^2 - (\sigma_0^{(2)})^2] + \frac{1}{4k_BT}[(\sigma_0^{(1)})^2 + (\sigma_0^{(2)})^2]\frac{f_n(\epsilon_0)}{f_n(\epsilon_0)-f_n(\epsilon_\infty)}\frac{Q_1+Q_2}{Q_1-Q_2}. \tag{46}$$

We have used Eq. 10 to relate $\alpha_{\rm tot}$ to α_0, and Eq. 34 to relate α_0 to the cavity sizes. After a little algebra, we find

$$\sigma_0^{(1)} = \sqrt{2k_BT(\lambda+\Delta G_{21})/\left(1+\frac{f_n(\epsilon_0)}{f_n(\epsilon_0)-f_n(\epsilon_\infty)}\frac{Q_1+Q_2}{Q_1-Q_2}\right)} \tag{47a}$$

and

$$\sigma_0^{(2)} = \sqrt{2k_BT(\lambda-\Delta G_{21})/\left(1-\frac{f_n(\epsilon_0)}{f_n(\epsilon_0)-f_n(\epsilon_\infty)}\frac{Q_1+Q_2}{Q_1-Q_2}\right)}. \tag{47b}$$

Using the same values for $f_n(\epsilon_0)$ and $f_n(\epsilon_\infty)$ as before, these equations predict $\sigma_0^{(1)} = 1.3$ kcal/mol and $\sigma_0^{(2)} = 1.0$ kcal/mol. These widths are also far narrower than the widths observed in the simulations.

It seems that it is not possible to use the simple dielectric continuum theory we have described to predict spectral line shapes in accord with simulation results. We need to employ a non-linear cavity size correction to account for electrostriction of the solvent by the solute molecule. Thus, the cavity radius decreases when the solute is made more polar. When we are consistent in the calculation of solvent fluctuations, however, the fluctuations predicted by the theory with the cavity size corrections are smaller than the fluctuations observed in computer simulations. Thus, the dielectric continuum theory seems to predict a greater degree of dielectric saturation than is actually observed.

V. CONCLUSION

In this paper we have explored the implications of a simple linear response, dielectric continuum for the dependence of absorption and fluorescence spectra on the polarizability of the solvent. The theoretical predictions have been tested using simulations of two electronic states of formaldehyde in polarizable and non-polarizable water. An important parameter describing the solvation is the reorganization energy, which measures the difference in the solvation of the two solute states. In the simulations, we found that the ratio of reorganization energies in polarizable versus non-polarizable solvents was 0.94 ± 0.05. The theoretical prediction, based on the assumption of a common cavity size for the ground and excited states of formaldehyde, is a ratio of 0.71.

We have reformulated the theory to allow for changes in the effective solute radius. When this is done, and the cavity radii are obtained from the solvation structure in the simulation, the theoretical prediction for the ratio of reorganization energies is 0.86, much closer to the simulation results. We are confident that even better agreement would be obtained if we extended our theory to include a coupling between the solvent and the quadrupole moment of the solute and used realistic nonspherical cavity geometries. This is because the difference between reorganization energies in polarizable and non-polarizable solvents becomes less pronounced as interactions with higher order multipoles are considered.

We find, however, that the non-linear corrections needed to obtain good results for reorganization energies have an

undesired effect on the linewidths predicted for the absorption and fluorescence spectra. The lines turn out to be far narrower than seen in the simulations, indicating that the dielectric continuum theory underestimates the solvent fluctuations. Therefore, it does not seem possible for a single, self-consistent dielectric continuum theory to describe properly all aspects of solvation.

Our work has a clear implication for simulation studies of related processes, such as charge transfer reactions, in non-polarizable solvents. In a charge transfer reaction, the activation energy is given in the Marcus picture by $E_{\rm act}=(\Delta G+\lambda)^2/4\lambda$, where ΔG is the free energy difference between reactant and product and λ is the reorganization energy for the reaction. It seems clear that if λ is measured in a simulation using a non-polarizable solvent, then it must be reduced by some scaling factor to account for the implicit (and incorrect) contributions from high-frequency electronic polarization modes. Such a rescaling has been attempted, for instance, in a recent large-scale simulation study of the photosynthetic reaction center.[12] Our work indicates, however, that the exact value of the scaling factor might be quite difficult to estimate.

In contrast to predictions for the reorganization energy, which required different cavity sizes for the two solute electronic states, our results indicate that predictions for solvation free energies can be accurate with just a single cavity radius. This is an interesting point because the Poisson and Poisson–Boltzmann equations, which are mathematical formulations of dielectric continuum theory, are often used to mimic the effects of a real, molecular solvent. The continuum solvent in these applications is parameterized by a dielectric constant and the solute is represented as a charge distribution inside an excluded volume. Our results indicate that a parameterization based solely on equilibrium properties might fail when predicting properties such as reorganization energies. Furthermore, our results seems to indicate that it might be essential to allow the cavity describing a solute to depend on the charge distribution inside, resulting in a type of non-linear coupling between solute and solvent.

In a forthcoming work,[29] we describe the results of just such a study using PBF,[25] a program which provides a numerical solution for the Poisson–Boltzmann equation. The program was specially modified to allow the calculation of absorption and fluorescence peaks for a polarizable continuum solvent with the dielectric properties of TIP4P-FQ ($\epsilon_0=80$, $\epsilon_\infty=1.592$).[71] The simulation results described in this paper serve as a basis for judging the performance of the dielectric continuum solvent model. We found that PBF provided very good results for free energy differences, but the non-equilibrium reorganization energies did not agree with the simulation results.

It is interesting to note that there exists a continuum solvent model which in fact includes just this type of nonlinear coupling between solute and solvent, namely the RISM model with HNC closure which bears a strong resemblance to the Gaussian field theory described in Sec. II E. In the RISM/HNC method, the solute–solvent distance correlations depend self-consistently on the interaction potential. Thus RISM/HNC predictions automatically include nonlinear effects due to cavity size changes. Although the RISM/HNC equations can be difficult to solve, these integral equation methods have been applied in the context of charge transfer reactions.[74–76] A promising avenue is explored in Ref. 77, in which the full three dimensional geometry of the solute is maintained during the solution of the HNC equations (albeit with a fixed solute–solvent direct correlation function).

Finally, we note that the polarizability of the solute itself can also be important in understanding the energetics of solvation, as well as the dynamics.[78] The fluctuating charge method used here to simulation polarizable water is very well suited for simulation studies of polar molecules[30] and ions[79] in solution. Treatments of solute polarizability based on dielectric continuum theories are also possible.[80]

ACKNOWLEDGMENTS

B.J.B. wishes to acknowledge the Alexander von Humboldt Foundation for granting him a senior scientist research award. This work was also supported by a grant from the National Science Foundation No. NSF-CHE-91-22506. Portions of the computational work were performed on the Thinking Machines CM5 of the NIH Research Resource Center of the Columbia Center for Biomolecular Simulation.

APPENDIX: COUPLING $\mathscr{E}_0$ TO $\mathscr{E}_\infty$

The terms $\mathscr{E}_0$ and $\mathscr{E}_\infty$ in Eq. 1 represent solvent polarization arising from slow modes and fast modes. In a phenomenological model of the solvent polarization, these modes are coupled and a term $-k\mathscr{E}_0\cdot\mathscr{E}_\infty$ is included in H_B. In this Appendix, we show that the coupling serves only to redefine certain terms in the diabatic Hamiltonians of Eq. 3. Thus, including the coupling term does not alter any of our subsequent analysis.

Our starting point is the diabatic Hamiltonian for solute electronic state Q_i where $i=1$ or 2:

$$H_i=E_i-(\mathscr{E}_0+\mathscr{E}_\infty)\cdot Q_i+\frac{1}{2\alpha_0}\mathscr{E}_0^2+\frac{1}{2}\alpha_0\omega_0^2\Pi_0^2 - k\mathscr{E}_0\cdot\mathscr{E}_\infty+\frac{1}{2\alpha_\infty}\mathscr{E}_\infty^2+\frac{1}{2}\alpha_\infty\omega_\infty^2\Pi_\infty^2-\frac{1}{2}\hbar\omega_\infty. \quad \text{(A1)}$$

Since $\omega_\infty\gg\omega_0$, we can perform a Born–Oppenheimer separation. We assume that the mode $\mathscr{E}_\infty$ remains in its ground state. The diabatic Hamiltonian for the mode $\mathscr{E}_0$ is

$$H_i=E_i-(1+\alpha_\infty k)\mathscr{E}_0\cdot Q_i-\frac{1}{2}\alpha_\infty Q_i^2 + \frac{1}{2\alpha_0}(1-\alpha_0\alpha_\infty k^2)\mathscr{E}_0^2+\frac{1}{2}\alpha_0\omega_0^2\Pi_0^2. \quad \text{(A2)}$$

Now we make the substitutions $(1+\alpha_\infty k)\mathscr{E}_0\rightarrow\mathscr{E}_0'$ and $\alpha_0(1+\alpha_\infty k)^2/(1-\alpha_0\alpha_\infty k^2)\rightarrow\alpha_0'$. The new momentum Π_0' is $\partial H/\partial\mathscr{E}_0'=\Pi_0/(1+\alpha_\infty k)$. The frequency is also rescaled, $\omega_0^2(1-\alpha_0\alpha_\infty k^2)\rightarrow\omega_0'^2$. With these substitutions, the diabatic Hamiltonian is

$$H_i = E_i - \mathscr{E}_0' \cdot Q_i - \frac{1}{2}\alpha_\infty Q_i^2 + \frac{1}{2\alpha_0'}\mathscr{E}_0'^2 + \frac{1}{2}\alpha_0'\omega_0'^2\Pi_0'^2. \tag{A3}$$

Because we are treating the mode $\mathscr{E}_0$ classically, the frequency renormalization has no effect on any of the energies which are to be calculated. The effective Hamiltonian we have obtained is therefore identical with the diabatic states of Eq. 3.

[1] A. C. Shepard, Y. Beers, G. P. Klein, and L. S. Rothman, J. Chem. Phys. **59**, 2254 (1973).
[2] C. A. Coulson and D. Eisenberg, Proc. Roy. Soc. London, Ser. A **291**, 445 (1966).
[3] R. A. Marcus, J. Am. Chem. Soc. **24**, 966 (1956).
[4] R. A. Marcus, J. Am. Chem. Soc. **24**, 979 (1956).
[5] R. A. Marcus and N. Sutin, Biochim. Biophys. Acta **811**, 265 (1985).
[6] R. A. Marcus, Rev. Mod. Phys. **65**, 599 (1993).
[7] A. J. Leggett *et al.*, Rev. Mod. Phys. **59**, 1 (1987).
[8] A. M. Kuznetsov, J. Phys. Chem. **96**, 3337 (1992).
[9] R. A. Marcus, J. Phys. Chem. **96**, 1753 (1992).
[10] J. N. Gehlen, D. Chandler, H. J. Kim, and J. T. Hynes, J. Phys. Chem. **96**, 1748 (1992).
[11] J. N. Gehlen and D. Chandler, J. Chem. Phys. **97**, 4958 (1992).
[12] M. Marchi, J. N. Gehlen, D. Chandler, and M. Newton, J. Am. Chem. Soc. **115**, 4178 (1993).
[13] X. Song and R. A. Marcus, J. Chem. Phys. **99**, 7768 (1993).
[14] J. J. Zhu and R. I. Cukier, J. Chem. Phys. **102**, 8398 (1995).
[15] M. Born, Z. Physik **1**, 45 (1920).
[16] P. Debye, *Polar Molecules* (Dover, New York, 1929).
[17] L. Onsager, J. Am. Chem. Soc. **58**, 1486 (1936).
[18] J. G. Kirkwood, J. Chem. Phys. **7**, 911 (1936).
[19] H. Fröhlich, *Theory of Dielectrics* (Oxford University, Oxford, 1949).
[20] C. J. F. Bottcher, *Theory of Electric Polarization* (Elsevier, New York, 1978).
[21] J. Warwicker and H. C. Watson, J. Mol. Biol. **157**, 671 (1982).
[22] M. K. Gilson, K. A. Sharp, and B. Honig, J. Comput. Chem. **9**, 327 (1988).
[23] A. Nicholls and B. Honig, J. Comput. Chem. **12**, 435 (1991).
[24] B. Honig and A. Nicholls, Science **268**, 1144 (1995).
[25] C. Cortis and R. A. Friesner (in preparation).
[26] V. Mohan, M. E. Davis, J. A. McCammon, and B. M. Pettitt, J. Phys. Chem. **96**, 6428 (1992).
[27] S. W. Rick and B. J. Berne, J. Am. Chem. Soc. **116**, 3949 (1994).
[28] D. J. Tannor *et al.*, J. Am. Chem. Soc. **116**, 11 875 (1994).
[29] J. S. Bader and B. J. Berne (in preparation).
[30] S. W. Rick and B. J. Berne, J. Am. Chem. Soc. **116**, 3949 (1984).
[31] M. Sprik, M. L. Klein, and K. Watanabe, J. Phys. Chem. **94**, 6483 (1990).
[32] P. O. Astrand, A. Wallqvist, G. Karlstrom, and P. Linse, J. Chem. Phys. **95**, 8419 (1991).
[33] J. C. Shelley, M. Sprik, and M. L. Klein, Langmuir **9**, 916 (1993).
[34] J. S. Cao and B. J. Berne, J. Chem. Phys. **99**, 2902 (1993).
[35] J. Lobaugh and G. A. Voth, J. Chem. Phys. **100**, 3039 (1994).
[36] D. E. Smith and L. X. Dang, J. Chem. Phys. **100**, 3757 (1994).
[37] X. G. Zhao and R. I. Cukier, J. Phys. Chem. **99**, 945 (1995).
[38] M. H. New and B. J. Berne, J. Am. Chem. Soc. **117**, 7172 (1995).
[39] S. W. Rick, S. J. Stuart, and B. J. Berne, J. Chem. Phys. **101**, 6141 (1994).
[40] W. L. Jorgensen *et al.*, J. Chem. Phys. **79**, 926 (1983).
[41] J. T. Blair, K. Krogh-Jespersen, and R. M. Levy, J. Am. Chem. Soc. **111**, 6948 (1989).
[42] J. T. Blair, R. M. Levy, and K. Krogh-Jespersen, Chem. Phys. Lett. **166**, 429 (1990).
[43] R. M. Levy, D. B. Kitchen, J. T. Blair, and K. Krogh-Jespersen, J. Phys. Chem. **94**, 4470 (1990).
[44] J. Ulstrup, *Charge Transfer Processes in Condensed Media* (Springer, New York, 1979).
[45] P. G. Wolynes, J. Chem. Phys. **87**, 6559 (1987).
[46] A. Warshel, Z. T. Chu, and W. W. Parsons, Science **246**, 112 (1989).
[47] J. S. Bader, R. A. Kuharski, and D. Chandler, J. Chem. Phys. **93**, 230 (1990).
[48] D. Chandler, in *Liquids, Freezing and Glass Transition, Les Houches, Session LI, 1989*, edited by J. P. Hansen, D. Levesque, and J. Zinn-Justin (North-Holland, New York, 1991).
[49] X. Song and A. A. Stuchebrukhov, J. Chem. Phys. **99**, 969 (1993).
[50] R. Egger and C. H. Mak, J. Chem. Phys. **99**, 2541 (1993).
[51] K. Sharp and B. Honig, Annu. Rev. Biophys. Biophys. Chem. **19**, 301 (1990).
[52] J. S. Bader and B. J. Berne (in preparation).
[53] Y.-P. Liu and M. D. Newton, J. Phys. Chem. **98**, 7162 (1994).
[54] B. Jayaram, R. Fine, K. Sharp, and B. Honig, J. Phys. Chem. **93**, 4320 (1989).
[55] H. Li and M. Kardar, Phys. Rev. Lett. **67**, 3275 (1991).
[56] H. Li and M. Kardar, Phys. Rev. A **46**, 6490 (1992).
[57] D. Chandler, Phys. Rev. E **48**, 2898 (1993).
[58] G. Hummer, L. R. Pratt, and A. E. Garcia, J. Chem. Phys. (in press).
[59] L. R. Pratt (personal communication).
[60] J. S. Bader and B. J. Berne (in preparation).
[61] M. J. Neumann, J. Chem. Phys. **85**, 1567 (1986).
[62] S. J. Weiner, P. A. Kollman, D. T. Nguyen, and D. A. Case, J. Comput. Chem. **7**, 230 (1986).
[63] D. Van Belle and S. J. Wodak, J. Am. Chem. Soc. **115**, 647 (1993).
[64] K. Kondo and T. Oka, J. Phys. Soc. Jpn. **15**, 307 (1960).
[65] A. D. Buckingham, D. A. Ramsey, and J. Tyrell, Can. J. Phys. **48**, 1242 (1970).
[66] D. E. Freeman and W. Klemperer, J. Chem. Phys. **45**, 52 (1966).
[67] V. T. Jones and J. B. Coon, J. Mol. Spectrosc. **31**, 137 (1969).
[68] G. Ciccotti, M. Ferrario, and J. Ryckaert, Mol. Phys. **47**, 1253 (1982).
[69] H. C. Andersen, J. Comput. Phys. **52**, 24 (1983).
[70] M. P. Allen and D. J. Tildesley, *Computer Simulation of Liquids* (Oxford University, New York, 1987).
[71] R. A. Kuharski *et al.*, J. Chem. Phys. **89**, 3248 (1988).
[72] H. H. Jaffe and M. Orchin, *Theory and Applications of U.V. Spectroscopy* (Wiley, New York, 1962).
[73] These modifications to the program PBF were performed with the kind and invaluable assistance of C. Cortis.
[74] R. A. Kuharski and D. Chandler, J. Phys. Chem. **91**, 2978 (1987).
[75] I. Bhattacharya-Kodali and G. A. Voth, J. Phys. Chem. **97**, 11 253 (1993).
[76] S.-H. Chong, S.-I. Miura, G. Basu, and F. Hirata, J. Phys. Chem. **99**, 10 526 (1995).
[77] D. Beglov and B. Roux, J. Chem. Phys. **103**, 360 (1995).
[78] B. D. Bursulaya, D. A. Zichi, and H. J. Kim, J. Phys. Chem. **99**, 10 069 (1995).
[79] S. J. Stuart and B. J. Berne (in preparation).
[80] K. Sharp, A. Jean-Charles, and B. Honig, J. Phys. Chem. **96**, 3822 (1992).
[81] A. D. Buckingham, Proc. R. Soc. London, Ser. A **238**, 235 (1956).
[82] K. Krynicki, C. D. Green, and D. W. Sawyer, Discuss. Faraday Soc. **66**, 199 (1978).
[83] J. Jonas, T. DeFries, and D. J. Wilber, J. Chem. Phys. **65**, 582 (1976).
[84] K. Watanabe and M. L. Klein, Chem. Phys. **131**, 157 (1989).